Droplet microfluidic platform for fast and continuous-flow RT-qPCR analysis devoted to cancer diagnosis application

I Hajji, M Serra, L Geremie, I Ferrante, R Renault, J.-L Viovy, S Descroix, Davide Ferraro

Droplet microfluidic platform for fast and continuous-flow RT-qPCR analysis devoted to cancer diagnosis application

I. Hajji[a,b], M. Serra[a,b], L. Geremie[a,b], I. Ferrante[a,b], R. Renault[a,b], J.-L. Viovy[a,b], S. Descroix[a,b], D. Ferraro[a,b,c*]

[a] Laboratoire Physico Chimie Curie, Institut Curie, PSL Research University, CNRS UMR168, Paris, France

[b] Institut Pierre-Gilles de Gennes, Paris, France

[c] Dipartimento di Fisica e Astronomia G. Galilei, Università di Padova, via Marzolo 8, 35131 Padova, Italy

*corresponding author: Davide Ferraro (davide.ferraro@unipd.it); Stephanie Descroix (stephanie.descroix@curie.fr)

Abstract

RT-qPCR represents a key method in cancer diagnostic, however the constant increase in patients and cancer biomarker panels to screen requires the implementation of faster approaches allowing smaller reagents and samples volumes consumption. To fulfil these needs, we present here a fully automated droplet microfluidics platform that couples a specifically designed thermal system with a fluorescent excitation/detection module. Additionally, the droplet generation and merging approaches allows the analysis of multiple samples and genes with no risk of contamination. This platform has been initially validated by investigating HER2 overexpression in two cancer cell lines starting from total RNA samples; these results have been successfully compared with those obtained by a commercially available machine, showing no limitation in terms of number of processed samples as well as reducing 200 times the analysis costs per patient. Finally, we have demonstrated its capability in performing fast RT-qPCR, raising the throughput of analysis to a hundred samples in less than 20 minutes.

1 Introduction

Recent progresses in genomics led to a deep knowledge of tumour cells genetic characteristics, allowing to identify mutations specific to a particular cancer subtype and, in some cases, to devoted therapies[1]. This approach, defined as precision medicine[2] by the Food and Drug Administration (FDA), is nowadays a common practice in cancer diagnostics and clinics. A typical example for this methodology is the status of HER2 (Human Epidermal growth factor Receptor 2) gene in breast cancer, which presents an overexpression (HER2+ status) in 15-20% of primary breast cancers[3] and is associated with an aggressive tumour. However, recently the patients' outcome has been drastically improved by the administration of targeted treatments (e.g. Trastuzumab and Pertuzumab)[4].

The number of identified mutations is continuously increasing, thus the physicians must deal with larger gene panels to be analysed requiring higher sample amount, as well as larger reagents volumes leading to higher costs. To face these needs, new technologies must be developed allowing fast and multigene analysis of patient tumour while consuming a minimal amount of biological material. Current gold standards to achieve precision medicine diagnosis of breast cancer are Immunohistochemistry (IHC), Fluorescent In Situ Hybridization (FISH) and Reverse Transcription-Quantitative Polymerase Chain Reaction (RT-qPCR)[5]. All these techniques are based on the

screening of specific proteins or nucleic acids expressed in the cancer cells, which are known to be markers for a specific cancer subtype or associated with potential targeted therapy. Despite RT-qPCR methodology is quantitative, highly reliable and more labour-saving than other strategies[6], it remains rather expensive, notably due to the cost of reagents and because all the PCR-based diagnosis approaches require rigorous procedures and environments, in order to avoid contamination[7,8] and sample degradation, which is particularly critical for RNA analysis[9]. Therefore, the implementation of these bioanalytical methods in a microfluidic format has a great potential to overcome current limitations, as already attested by the approaches developed so far. The pioneer work of Quake et al.[10] presented a system for quantitative RT-PCR based on integrated PDMS valves, currently commercialized as IFC module by Fluidigm. Unfortunately, this disposable and expensive device processes a fixed number of samples per run (48 or 96), therefore it is not well-adapted to a clinical environment, where the samples number varies on a daily basis and the cost per run cannot be optimized. Droplet microfluidics[11,12] has the potential to bypass these limitations, guaranteeing stable compartmentalization without complex valve systems and, especially, using reusable devices since the droplets containing the samples never touch and contaminate the channel walls[13].

Nowadays, droplet microfluidics is well established for droplet-digital PCR protocols[14–16] (ddPCR), which consists in single molecule or cell encapsulation in droplet, thermal-cycling amplification and final endpoint detection. However, despite ddPCR allows to achieve single molecule analysis, required for example in circulating tumour DNA detection[17], it provides comparable results in term of sensitivity regarding the quantification of the expression level of target genes[18,19] that, as introduced above, represents the key aspect in current diagnostic strategies. Additionally, high level of multiplexing remains rather problematic due to false positive results[20,21]. Therefore, considering also its higher cost[18], ddPCR is still limited to research purposes and it is not yet diffused towards clinical laboratories[22], in which, common RT-qPCR technology is widely used. Unfortunately, droplet microfluidic devices devoted to the latter protocol are much less common. This is partially due to some technological challenges: differently from ddPCR, requiring one single endpoint detection[23,24], qPCR needs accurate and comparable fluorescent detection after each thermal cycle. Some examples reporting qPCR in droplets circumvent this issue by parking the droplets in a specific area of a microfluidic chamber[25–29] or on a EWOD device[30], performing the fluorescent analysis on stationary compartments[31]. Such approaches strongly limit the number of processed samples per run. Moreover, these devices are typically coupled with a fluorescent microscope, preventing their use away from an equipped laboratory and increasing the total cost for the experimental setup[25,26,32].

An interesting approach has been proposed by Hatch et al.[33] demonstrating continuous flow qPCR in droplets, generated by a T-junction. Despite this work represents the first proof-of-concept in the field, it suffers from several limitations. The sample preparation step is manually performed off-chip, strongly limiting the automation and the eventual capability for multiple gene analysis. Then, besides the large droplet volume (μL range), the optical module shows low excitation light homogeneity, leading to important issues in the fluorescent detection. The latter has been solved by drastically increase the fibers numbers and using high-sensitivity cameras[34], thus increasing the overall complexity and cost of the setup.

In this work, we present a droplet microfluidic platform, named Drop-qPCR, in which droplets, transported in a reusable capillary, alternatively flow through two areas kept at different constant temperatures[35], while the fluorescent detection is performed by a devoted system obtained by widespread and low-cost technologies: 3D printing, LEDs and a CMOS USB-camera. Additionally, Drop-qPCR allows automated analysis of different

combinations of samples and genes, thus guaranteeing perfect compatibility with conventional diagnostic protocols. In particular, the implemented droplet generation approach allows to sequentially produce pairs of droplets (sample and Master Mix) that spontaneously merge exploiting their difference in interfacial tension[36]. To evaluate the potential of the Drop-qPCR platform, it has been successfully compared with a commercial RT-qPCR equipment, showing the capability of performing analysis with throughput competitive with the current microfluidic ultrafast-qPCR system[32], which however is not based on droplets microfluidics. Finally, this platform implements for the first time the complete RT and qPCR protocol, thus starting from total RNA samples which, as mentioned before, are very delicate and prone to degradation. This represents an important skill for its implementation in routine clinical practice.

In the following, we first describe the technological development of the platform and its characterization. Then, Drop-qPCR is validated i) by determining the expression level of the HER2 gene starting from total RNA samples extracted from cancer cell lines and ii) by comparing the obtained results with a commercially available qPCR system. Finally, we evaluate and discuss the analytical throughput achievable by the developed technology, compared to state-of-the-art microfluidic strategies.

2 Materials and Method

The Drop-qPCR platform is composed by several modules. Some of them have been developed during this work and will be described in the "Results and discussion" section, while others that are commercial or have already been presented in previously published works, will be introduced in the following.

The droplet generation system, presented in[37], is composed by an arm-robot (Rotaxys, by Cetoni) coupled with two syringe pumps (Nemesys, by Cetoni) mounting two syringes (2.5mL and 250µL, by SGE) and two customized pinch valves[38]. Aqueous phase droplets are thus generated by pipetting in fluorinated oil (FC40, by 3M) with 2% w/w of a fluorinated surfactant (1H, 1H, 2H, 2H-perfluoro-1-decanol, by Fluorochem) and transported in PTFE capillary (0.3mm/0.6mm inner/outer diameter, by Sigma Aldrich). Notably, the use of a fluorinated oil (FC-40) mixed with fluorinated surfactant assures a complete wetting of the fluorinated capillary, preventing any cross-contamination during the pipetting[37]. This will be additionally confirmed by the qPCR results from the setup validation. Liquids used for droplet generation (aqueous and oil phases) are stored in a commercial 384-wells microtiter plate (AB1384Y, by Thermofisher).The different parts of the RT and qPCR modules, that are detailed in the Results and Discussion paragraph, have been produced by micro-milling using the Mini-Mill machine (by Minitech) or 3D printing, by using acrylonitrile butadiene styrene (ABS) plastic and DL-260 resin (by DWS Systems). uPrint SE Plus (by Stratasys) and DigitalWax028J+ (by DWS Systems) printers are used for the two materials in order to obtain low and high resolution parts[39], respectively.

For temperature control and monitoring, Peltier modules (CP2-127-06L, by Laird Technologies) controlled by three independent PID boards (TC M PCB by Electron Dynamics) are coupled with three thermal sensors (PT100, by RS Pro) placed in correspondence to the heated parts. All the surfaces in contact that require a good heat exchange are firstly covered with thermal paste (by RS Pro). The temperature characterisation is performed with small-sized thermocouples (0.23mm, IT-24P, by PHYMEP) inserted in the PTFE capillary.

For the fluorescence detection part, several optical components have been used: LEDs (CP7P-GZHX-1, by OSRAM), aspheric and cylindrical lenses (354140-A and LJ1598L1-A, by Thorlabs), filters (excitation 485/20 nm and emission 530/43nm, by Semrock) and a macro-lens (MLV7000, by Navitar) installed on a camera (acA2500-60um, by Basler). The acquisition framerate is set in between 20fps and 40fps according with the applied flowrate, in order to assure a correct visualization of the flowing droplets. The spectral filters are chosen in agreement with the Taqman probe used during the qPCR experiments (FITC filter set).

Finally, the total RNA samples used during the RT-qPCR analysis are extracted from two human cell lines SKBR3 (ATCC® HTB-30™) and MCF7 (ATCC® HTB-22™) by spin columns method (RNeasy Mini Kit by Qiagen). The Master Mixes, containing primers for the two investigated genes (HER2 and Actin-β, or ACTB) and Taqman probe, are prepared using the CellsDirect™ One-Step qRT-PCR Kit (by Thermo Fisher Scientific) as indicated in ESI (see Note S1), for both in-droplet experiments and commercial qPCR machine (SmartCycler II, by Cepheid). Each RT-qPCR analysis is repeated at least twice for each sample. The kit has been chosen because it allows both RT and qPCR from the same reaction solution. In detail, the PCR requires incubation times at two temperature conditions (denaturation at T=95°C, annealing and elongation at T= 60°C).

3 Results and discussion

3.1 Drop-qPCR platform development

The droplet microfluidic platform is composed by three sequential modules for the implementation of three different tasks: i) droplet generation, ii) Reverse Transcription (RT) and iii) qPCR. The first module, already presented in[37,40], allows the pipetting of deterministic trains of confined droplets (between 50 and 300nL, volume polydispersity <2%) from solutions stored in a conventional microtiter plate (see Figure 1a). This approach provides high flexibility in programming the droplet content, which can be tuned by adjusting the pipetting sequence. Additionally, the microtiter plate and capillary used ensure a minimal waste of reagent that stay on the bottom of the well of 200nL (see Note S2 in ESI). Moreover, due to a combination of pinch valves and PDMS devices[37], droplets generation can be performed while other droplets previously prepared are flowing in the microfluidic device for the analysis. This allows to achieve a throughput which is not limited by the droplet generation. Additionally, due to the combination of oil and capillary used, possible contaminations between the different wells of the microtiter plate during the droplets sampling are prevented, as demonstrated in[37]. Finally, this system enables decoupling the droplets generation and their processing in the platform, allowing: i) the parallelization between samples pipetting and analysis; ii) the control of the carrier liquid flowrate, keeping constant the droplets size and the production rate.

During the experimental protocol, pairs of droplets (volumes of 100nL), containing respectively total RNA sample and RT-qPCR Master Mix, are continuously generated. In parallel, to fulfil the clinical requirements, negative controls are also analysed during the experiments. These can be easily implemented in the Drop-qPCR platform by pipetting a water droplet instead of the total RNA sample. To induce the sample and the Master Mix droplets merging, we have taken advantage of the interfacial tension difference between each droplet and the carrier fluid (12.8±0.5mN/m and 2.9±0.2mN/m, respectively). As described in[36], when a confined droplet is transported by a carrier fluid, its speed is a function of the interfacial tension (γ) between the two liquids; notably,

lower γ leads to higher speed. Therefore, this effect has been exploited to induce a spontaneous droplets contact and thus, their merging after a constant travelled distance (15cm±1cm, see also ESI in [36]). Notably, being based on the different interfacial tensions of the droplets with the oil phase, this approach ensure 100% merging efficiency, as experimentally observed.

After the merging, the resulting daughter droplets flow in the second module devoted to the RT reaction, at a flowrate of 120nL/s. This module is designed to incubate the flowing droplets at a fixed temperature for a desired time, at 50°C for 11 minutes in this case. Therefore, as shown in Figure 1b, we have developed a RT module composed by a brass part presenting a groove on its surface with a serpentine design that acts as capillary holder. In order to assure the desired homogeneous temperature on the capillary, the brass plate is fixed on the Peltier module which is coupled with a heatsink for the temperature dissipation. Finally, an ABS 3D-printed lid is placed all around the module to guarantee thermal insulation from the external environment[41].

After the RT, droplets containing the resulting cDNA continuously flow in the third module dedicated to PCR amplification and real-time fluorescence detection. This module allows both temperature cycling and fluorescence measurements after each cycle and for each droplet. These two sections will be separately discussed in the following.

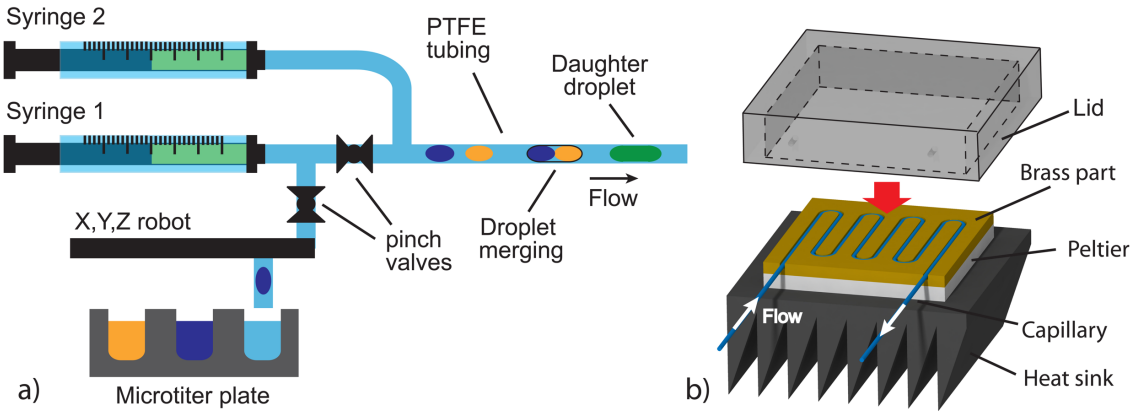

Figure 1: a) Module for droplet generation and flow (module 1). Two pinch-valves connected with two syringe pumps guarantee a continuous pairs of droplets generation starting from solutions stored in a microtiter plate. The first droplet (yellow) contains the RNA sample and the second (blue) the Master Mix for the RT-qPCR. After the generation, droplets are transported in the capillary towards the 2nd module of the platform; during the flow, each pair spontaneously merges resulting in a daughter droplet (green) ready for the RT protocol. (b) Scheme of the RT module (module 2): droplets experience a constant temperature (50°C) flowing in the capillary placed inside the brass part and then, they are transported to the 3rd module for the qPCR amplification.

qPCR module: Thermal cycling

As shown in Figure 2a, the third module of the platform is composed by two heating parts facing each other, independently assembled and controlled, as for the RT module. The same capillary (approximatively 5m long) is thus rolled-up in between the two parts in order to let the flowing droplets experience two temperatures in alternate manner. This arrangement allows the production of a more compact device than using the common flat configuration[15]. More details about the capillary installation are reported in ESI (see Note S3 and Figures S1,S2). Additionally, in order to guarantee a homogeneous temperature around the capillary, we have designed the brass plates with 45 straight and parallel pockets on the surfaces, having squared cross section (see Figure

2b). Then, the two faced heating parts are held together by two screwed 3D printed structures, reported as dashed rectangles in Figure 2a. In detail, a first U-shaped structure (left side in Figure 2a) fixes the plates position and keeps them at a mutual distance of 1cm. Then, a second structure (right side in Figure 2a) presents a comb-like shape in which the capillary is passed through, as shown in Figure 3a. These 45 vertical windows, aligned with the pockets on the brass parts, assure the optical accesses required for the fluorescence measures.

Once the thermocycling part is assembled, we have verified the temperature homogeneity and stability by inserting different thermocouples in the capillary hosted by the brass plates. As shown in Figure 2c, the device takes about 4 minutes to reach the desired temperature and presents an average oscillation of 0.2°C. These are crucial requirements for a proper DNA amplification; in fact, enzymes and primers involved in the annealing step are designed to work at specific temperatures and any divergence may lead to low amplification efficiency (<90%)[42,43].

Therefore, by keeping the two brass parts at the temperatures required for the amplification protocol, droplets experience the 45 temperature cycles just flowing in the capillary. In detail, the experiment is designed to keep them 25s at both 60°C and 95°C by applying a constant flowrate of 120nL/s, which allows to perform a complete PCR cycle in approximately 1 minute. These times have been calculated as the ratio between, the width of the brass plate multiplied by the capillary section, and the flowrate.

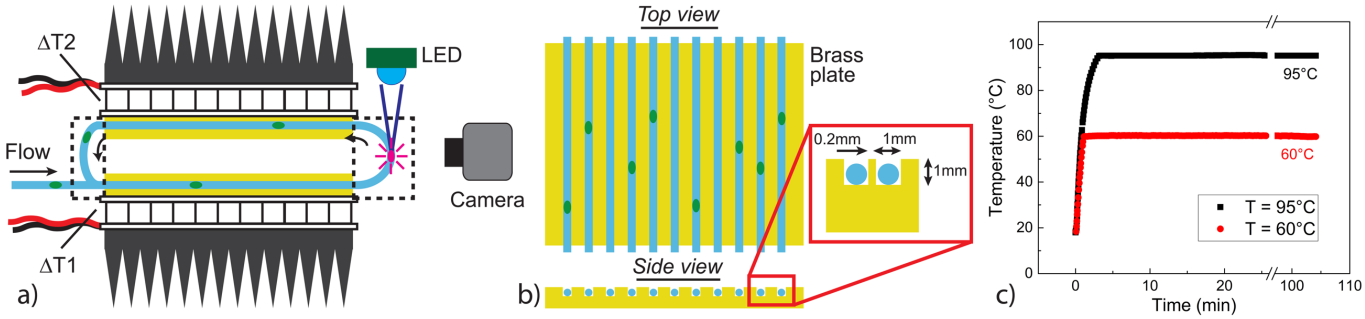

Figure 2: qPCR module – thermal cycling part. a) The capillary (light blue) is rolled-up in between two brass plates (yellow) kept at defined temperatures; b) the plates present straight and parallel pockets holding the capillary in a homogeneous temperature environment. c) Temperatures monitoring on both brass plates: denaturation part (95°C, black dots) and annealing-extension (60°C, red dots). These measurements are performed by thermocouples placed in a capillary installed in the device and the time=0min corresponds to the device starting.

qPCR module: Fluorescence optical measurement

Typical qPCR curves are obtained in a commercial machine by performing a fluorescence measure of the sample between each amplification cycle. Therefore, the same approach has been applied in the microfluidic device: the detection is done in between every droplet turn in the capillary, which corresponds to a PCR cycle.

The fluorescence measure is performed through the observation windows integrated in the 3D printed part as previously described (Figure 3a). More in detail, the excitation light is focused on the capillary's portions passing through the observation windows and the subsequent droplet fluorescence emission is collected by the camera placed in front of it (see Figure 2a). Thus, knowing the droplet generation order, the qPCR curve is easily obtained for each one, by plotting its fluorescence intensity versus the turn (or cycle) number. Notably, camera and macro-lens have been chosen (see Material and Methods) in order to assure a field of view large enough to observe all the 45 observation windows in the same frame.

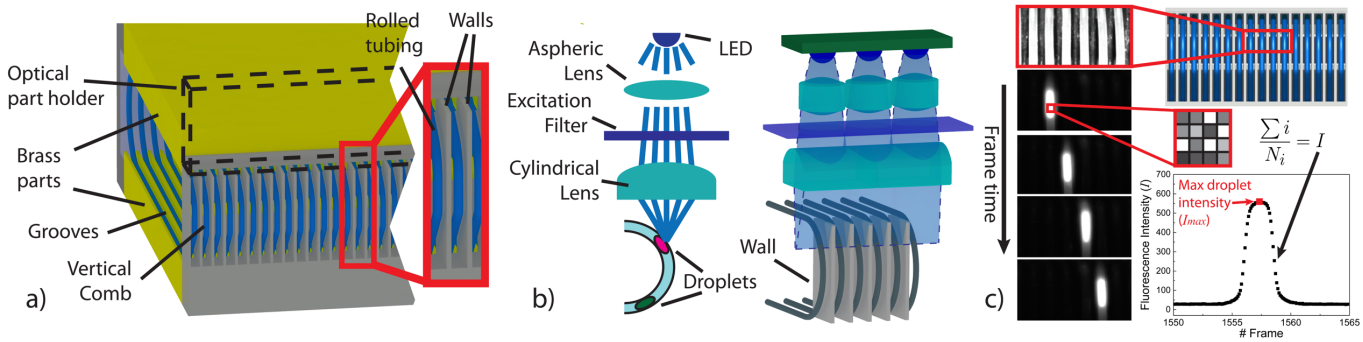

Figure 3: scheme of the module 3. a) A 3D printed comb-like structure (grey) fixes the positions of the capillary on which the optical fluorescence detection takes place. This part is designed to be aligned with the pockets of the brass plates and to avoid light pollution between capillary turns during the detection. b) Scheme of the optical path followed by the LED light in order to obtain a beam homogeneously focused on a line. Optical components are designed to irradiate specific areas of the capillary, which are imaged by an external camera. c) Image processing workflow: for all the images, a ROI is defined for each capillary turn and its average pixel intensity value (I) is constantly monitored; when the droplet crosses the detection window, a peak is observed and its maximum is taken as the fluorescence intensity value of the droplet (Imax). To better visualize the droplet in the figure, in the images' sequence, a saturated fluorescent image has been considered. See Movie S1 to view an example of an acquisition of a quantitative experiment.

Since the fluorescence emission is proportional to the excitation light intensity, in order to compare the signals coming from the different observation windows, thus from different PCR cycles, a homogenous irradiation is required. This has been achieved by combining a custom-made optical setup and a post-processing signal analysis algorithm. In detail, the setup is composed of a series of optical components aligned by a devoted micro-milled structure, which is installed on top of the comb-like structure (see dashed line in Figure 3a and Figures S3,S4 in ESI). As reported in Figure 3b, the light emitted by an array of 13 LEDs (peak emission centre 465 nm) is collected by 13 aspheric lenses; each LED-lens couple is placed in contact between each other in order to collect all the light emitted by the LED. Being this distance smaller than the focal length of the aspheric lenses used (1.45mm), a divergent light is obtained which is, at first, narrowed by a FITC excitation filter (485/20 nm), then focalized by cylindrical lenses. The distance between the aspheric and cylindrical lenses has been experimentally optimized at 4.5 mm, in order to collect all the light. Therefore, this optical structure is designed to collect the initial LED light and to produce an elongated and homogenous beam, minimizing light loss, as typically obtained by using conventional diffuser. Finally, an emission FITC filter (530/43nm) is installed in between the macro-lens and the camera, to increase the signal/noise ratio. In this way, it is possible to continuously record the entire region exposed to the excitation beam and to visualize the fluorescence emission of the droplets flowing in the capillary (see Movie S1 in ESI). Importantly, since every portion of the capillary is embedded in the comb-like structure (see Figure 3a), the walls act as optical insulators between the different observation windows (pictures of the setup are reported in Figure S4 in ESI).

The acquired images are then analysed by a dedicated Matlab program. In each frame, 45 regions of interest (ROIs, 170x170µm²) are univocally associated to each of the 45 capillary portions, corresponding to the 45 amplification cycles, as shown in Figure 3c. Therefore, for each frame the system allows to monitor in parallel all the ROIs by measuring the fluorescence signal; the average pixel value (I) in the ROI is plotted as function of the acquisition time. Initially, a constant background value is measured, then, when the droplet crosses the ROI, a peak is observed as shown in Figure 3c and in Movie S1 (see ESI). The peak maximum I_{max} is the representative value for the fluorescence intensity of a droplet in a given ROI, thus for the corresponding thermal cycle. Notably,

by using a Taqman probe, which presents an initial detectable fluorescence signal, all droplets are discerned starting from the first cycle therefore, being confined and preserving their generation order, they are also univocally identified by their ordinal number.

In order to evaluate the homogeneity of the excitation/emission light, a droplet containing a fluorescence calibration solution (400nM Taqman probe) is flown in the capillary recording its emission intensity from each ROI. A light uniformity higher than 82% is measured (see Figure S5 in ESI). Despite this represents a good result that does not involve customized devoted lenses[44,45], it is found to be not high enough to compare the emissions from the different 45 capillary's portions. However, since the unwanted light modulation represents a systematic error, a signal analysis post-processing has been applied to compensate this effect. In details, the signal from each ROI is systematically normalized by the emission intensity measured by the calibration solution, on the same ROI. In detail, 5 droplets of the calibration solution are flown in the capillary and the fluorescent signals from each ROI are acquired; the average values are then used to normalize all the measured intensities from the corresponding ROIs. Figure 4a reports two examples of qPCR curves before (top) and after (bottom) the normalization, respectively. Therefore, by plotting the normalized droplet intensity as function of the ROI number, we can achieve a conventional qPCR amplification curve of the corresponding sample. Finally, from this type of curves, the cycle threshold (or Ct) associated to the analysed sample can be easily extracted as for standard qPCR machines: the background probe signal is subtracted, resulting in curves aligned to the zero intensity, then the fluorescence threshold is chosen within the range of exponential phases of the amplification curves[46–49]. As a first proof of concept, Figure 4b reports data obtained with the Drop-qPCR platform for a sample of total RNA extracted from SKBR3 cell line and a negative control. These results prove the feasibility of the Drop-qPCR approach both in terms of DNA amplification and fluorescence detection. Finally, since the number of cycles required for observing the qPCR amplification curve depends on the initial quantity of targets, if less than 45 cycles are sufficient, the unnecessary last ROIs can be simply ignored during the data analysis, without requiring any adjustment in the setup nor extending the duration of analysis.

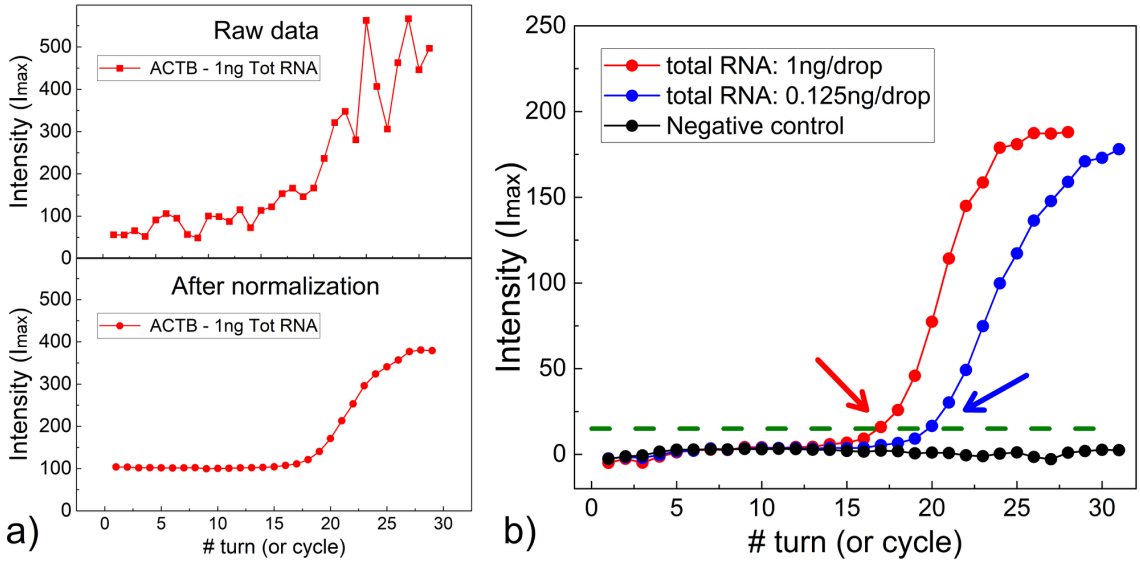

Figure 4: a) Plot of the fluorescence intensity (Imax) for each droplet as a function of the capillary turn number, corresponding to the amplification cycle, before(top) and after (bottom) the normalization; data are related to ACTB gene of Total RNA sample (1ng) from MCF7 cell lines (red). b) Examples of normalized and shifted qPCR curves obtained for the ACTB gene from the total RNA samples extracted from MCF7 cell lines at 1ng/drop (red dots) and 125pg/drop (blue dots), and negative control (black dots). The intersections between the threshold (green dashed line) and the amplification curves give the Ct values for each sample (red and blue arrows).

3.2 RT-qPCR analysis

To further evaluate the Drop-qPCR platform, analyses have been performed using total RNA samples extracted from two cell lines: SKBR3 and MCF7, that are known to overexpress and non-overexpress HER2, respectively[37]. In detail, these samples have been analysed in order to obtain calibration (or standard) curves for this gene, which is particularly relevant for breast cancer, using ACTB as reference gene. Such dual gene analysis allows to analyse the obtained data by the ΔCt method[50], which is typically applied to compare the gene expression across different samples or experimental conditions. Notably, for each calibration curve the droplets train is composed by 8 pairs of droplets: 7 for the two-fold dilutions of RNA (between 1ng/drop and 15pg/drop) and one negative control (DEPC-treated water). This range of concentration is lower than the typical quantities used for routine quality check of clinical samples (6 to 25ng per assay)[37] and the lowest calibration point (15pg/drop) corresponds to the average total RNA amount in a single cell.

Figure 4a reports the calibration curves for HER2 and ACTB genes in SKBR3 and MCF7 cell lines obtained using the Drop-qPCR. Each data point is the average result of the repeated experiments and the corresponding standard deviation is considered as the error bar. Coefficients of variation (CVs) are found always lower than 2.5%, showing an excellent repeatability. In order to evaluate the performance of the Drop-qPCR approach, the fit parameters, the coefficient of determination R^2, as well as the resulting PCR efficiencies, are summarised in Table 1. The calibration curves obtained for the total RNA extracted from the two cell lines (Figure 4a and Table 1) present a linear trend (R^2>0.95) and amplification efficiencies higher than 90%. These aspects are particularly important since they demonstrate that: i) the device design guarantees optimal and homogeneous thermal actuation and reliable fluorescence detection; ii) the results for the two investigated genes, can be analysed by ΔCt method. In fact, the latter can be applied only if the amplification efficiencies of the genes are comparable. Figure 4a also shows that the platform allows to clearly distinguish between 2-fold serial dilutions, which corresponds to the resolution limit of conventional qPCR assay[51]. Furthermore, considering the gene of interest for clinics (HER2), we observe that the MCF7 curve is shifted upward with respect to the SKBR3 one, indicating the expected overexpression of SKBR3. This is also shown by the resulting ΔCt values reported in the Table 1 ($\Delta Ct_{MCF7} > \Delta Ct_{SKBR3}$), confirming that Drop-qPCR allows to clearly differentiate between the two sample populations whatever the initial quantity of mRNA and down to single-cell level. Finally, since experiments are performed pipetting from the highest to lowest concentrations, plus a negative control, these results confirm that any cross-contaminations between the wells of the microtiter plate or droplets happened.

Furthermore, the performances of our device have been further evaluated by doing a systematic comparison between the data obtained by the Drop-qPCR and a commercially available qPCR system (SmartCycler II, by Cepheid). This comparison has been performed in the same conditions: genes, cell lines and initial quantity of total RNA. The obtained results show that the data by the Drop-qPCR platform and the SmartCycler are perfectly comparable (see Figure 4b and Table 1). In fact, both PCR efficiencies and ΔCt values for the two cell lines correspond within the propagated errors. This demonstrates that the droplet microfluidic platform provides an accurate quantification as the commercial system, despite the cost reduction in terms of reagents (Master Mix volumes reduction of 200 times). Finally, comparing Figures 4a and 4b, a decrease of about 6 Ct values is observed using the droplet platform. Since the fluorescence intensity of a molecule is proportional to its concentration, this effect is probably due to the total

RNA confinement in droplet, as already reported in micrometric size reaction chamber[52,53]. This may lead to the capability in detecting gene typically poorly expressed.

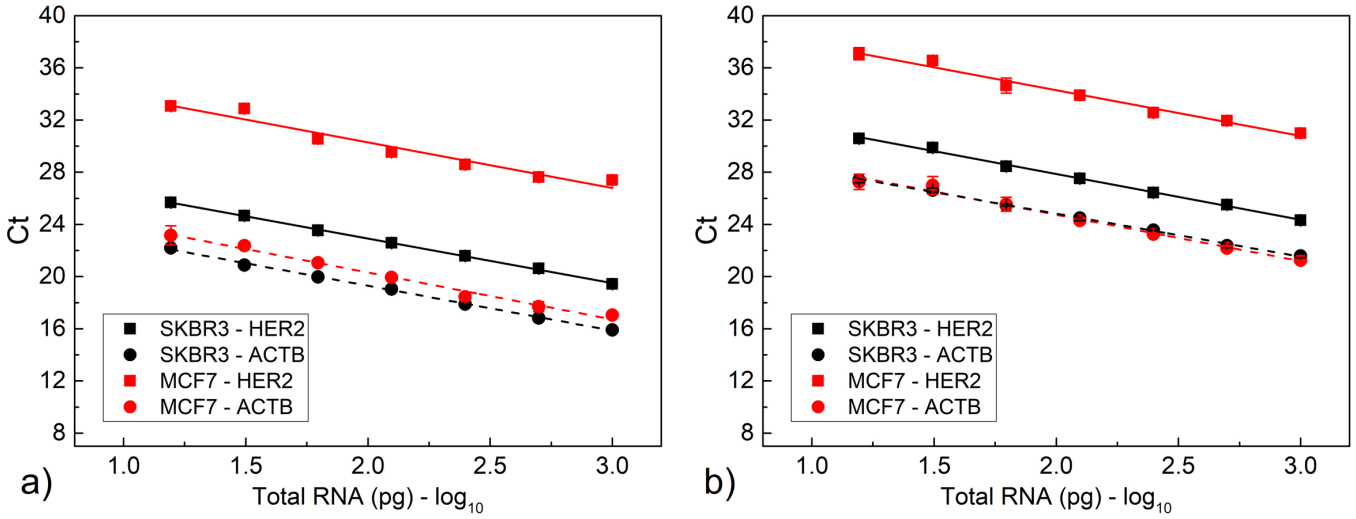

Figure 5: calibration curves obtained using the (a) droplet microfluidic device and the (b) commercial system (SmartCycler), using Total RNA sample extracted from MFC7 (red dots) and SKBR3 (black dots) cell lines, to determine HER2 (squared dots) and ACTB (circle dots) genes expression level. Error bars are not visible if smaller than associated data point. The solid and dashed lines are the linear fits of data related to the HER2 and ACTB genes, respectively. The parameters of the fits are reported in Table 1.

Table 1: Comparison of the results obtained in the droplet microfluidic platform and in the conventional qPCR machine. Investigated factors include fit parameters (Slope, Intercept and R2) of curves reported in Figure 4. PCR efficiencies and ΔCts.

			Slope	Intercept	R^2	PCR Eff.	ΔCt
Drop-qPCR	SKBR3	HER2	-3.42±0.04	28.75±0.08	0.998	96%	3.6±0.2
		ACTB	-3.44±0.06	25.18±0.14	0.997	95%	
	MCF7	HER2	-3.49±0.35	36.29±0.76	0.946	93%	9.8±0.8
		ACTB	-3.60±0.17	26.50±0.36	0.986	90%	
SmartCycler	SKBR3	HER2	-3.51±0.09	34.89±0.20	0.996	93%	3.5±0.2
		ACTB	-3.30±0.07	31.42±0.14	0.998	101%	
	MCF7	HER2	-3.51±0.21	41.30±0.45	0.980	93%	9.4±0.6
		ACTB	-3.56±0.17	31.86±0.37	0.987	91%	

3.3 Fast RT-qPCR evaluation

To investigate the analytical throughput of the Drop-qPCR platform, the workflows described above have been tested increasing the flowrate of the carrier oil between 150 and 600nL/s. In this way, droplets spend different residence times on the heating brass parts. Knowing the oil flowrate and the device geometry, the times required to perform one turn in the capillary, or one PCR cycle (cycling period), ranges between 47 and 12 seconds (see inset Figure 6a), corresponding to a residence time between 18.8 and 4.7 s at each temperature.

In order to quantitatively compare the different throughput conditions, Ct and amplification efficiency[47] are evaluated for a fixed total RNA quantity in 5 replicates (1ng of total RNA extracted from MCF7 cells for ACTB gene). Figure 6a reports the Ct values obtained as function of the flowrate. They are constant (average Ct=15.8) with CV<0.8% up to 450nL/s, while a higher Ct (=21.0) showing higher variability (CV=2.24%) is found at 600nL/s; this

indicates the upper speed limit of the protocol. Similarly, Figure 6b shows that PCR efficiencies and the related R^2 are constant within the error bars and present small CV (<5.3% and CV<0.1%, respectively) up to 450nL/s, while they decrease and are associated with higher variabilities (CV=13.7% and CV=1.7% respectively) at 600nL/s.

According to the heat exchanger model presented in[54], droplets experience a complete thermalization in less than 2 seconds for all investigated droplets' speeds. Since the shortest residence time on the brass part per cycle (for 600nL/s) is 4.7 seconds, the decrease in RT-qPCR performance at this flowrate is probably limited by the kinetics of the reactions: DNA denaturation (95°C) and/or annealing/elongation (60°C). According to general guidelines for nucleic acid amplification, the elongation time is the slowest and the limiting process. Similar limitation in time are also found in[32]. It is also worth noting that to get constant Ct values using the commercial qPCR machine (SmartCycler), at least 3 times longer cycling period have to be applied. This can be partially explained by the longer thermalization required for the larger reaction volume (25µL) and by the temperature ramp needed by the machine during the PCR cycles (see Note S4 and Figure S6 in ESI for more details).

Altogether, these results demonstrate that the Drop-qPCR platform allows performing the qPCR protocol (45 cycles) in less than 12 minutes (corresponding to a flowrate of 450nL/s and a cycling period of 15.7s), which not only is much faster than commercially available machines, but it is also consistent with the actual state-of-the-art in the monophasic microfluidic devices (cycling period: 14s)[32]. However, the latter is strongly limited by the number of samples that can be analysed per run; in fact, in order to parallelize the analysis for different samples, several disposable microfluidic chips must be employed. Differently, our platform allows sequential analysis of different samples, without presenting drastic limitation in the throughput. Additionally, once the droplets are generated and stored in the capillary at a mutual distance of 14 mm (corresponding of 1µL of oil), the time required for the total RT-qPCR analysis of 1 or hundred samples, differ of less than 5 minutes (15min for 1 sample and 20min for 100 samples).

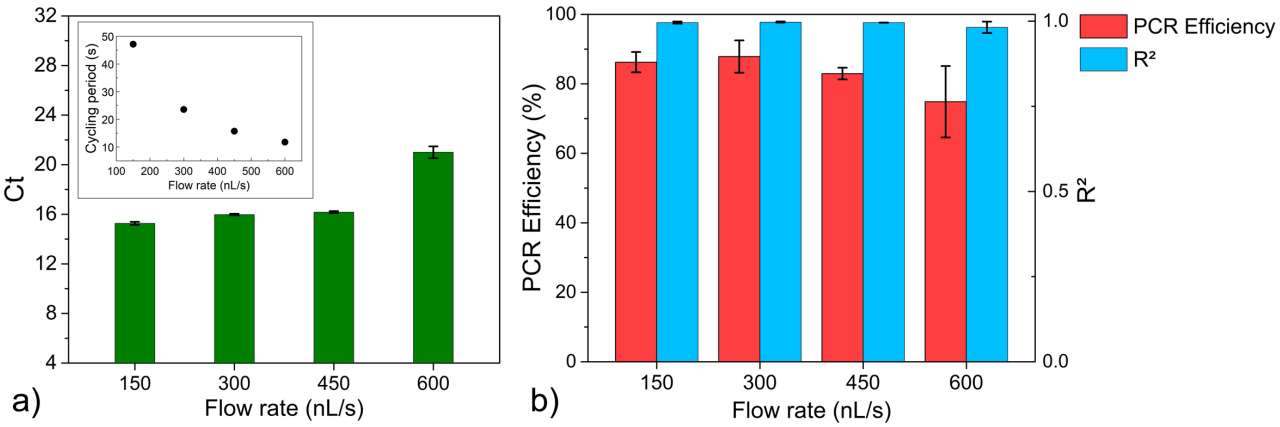

Figure 6: a)Cts, b)PCR Efficiency and related R^2 obtained for different flowrate conditions and thus, different cycling periods related to the qPCR (see a,inset). The results are consistent up to 450nL/s.

4 Conclusion

In this work, we present a novel microfluidic platform implementing samples and reagents merging, the entire RT and qPCR protocols, starting from total RNA samples. We demonstrated its ability to discriminate cells with different gene expression levels in perfect agreement with a commercial system, and despite a higher sensitivity and a 200-fold reduction in reagents volume. The latters allow fulfilling clinical laboratories needs in order to, respectively, i) increase the number of genes that can be screened starting from identical sample quantity and ii) reduce the cost per analysis, as it is mainly based on reagents consumption. Moreover, the Drop-qPCR was designed fully-automated and versatile to customize the number and the combinations of samples/genes, without the need for a trained user nor an external pipetting robot. Thus, leading to further cost reduction.

However, the increase in the gene panel per patient raise a major question of analysis duration. For that purpose, we showed that compared to other state-of-the-art systems, our platform presents the unique capacity of performing 30 qPCR cycles in less than 8 minutes for a single sample and in less than 12.5min for a hundred samples. Consequently, the Drop-qPCR is perfectly adapted to both small and large number of samples with fast analysis time, and thus being highly suitable for diagnosis applications.

Considering that the highest achievable throughput is limited by the kinetic of the PCR reaction, optimization in the reaction buffer solution [32,55] can represent important perspectives for further timing improvements of this technology. Finally, the lower RNA amount considered for the calibration curve corresponds to the one of a single cell (about 15pg/drop), thus future outlooks include the coupling of this technology with a single cell-encapsulation device [56].

, thus validating its suitability and potentialities for routine cancer screening in clinics. Notably, the results obtained are in perfect agreement with a commercial system, despite a strong reduction of both reagent and sample volumes required (up to 200 times). The latter is a crucial aspect in clinical laboratory in order to i) increase the number of genes that can be analysed starting from the same sample quantity and ii) reduce the cost per analysis, asnyrhfhngbf mainly based on the reagents consumption.

Additionally, Drop-qPCR has been designed to be a versatile tool allowing the automated screening of a customizable number and combinations of samples and genes, leading to a further reduction of costs in term of alternative pipetting robot or long manual operation performed by trained user. Then, the platform allows the application of the same pipeline used in diagnostic, which consists in multiple analysis per sample and negative control experiments. Moreover, to face the increasing number of gene panels to screen, the platform is able to perform hundred reactions in less than 20 minutes, presenting at the same time the unique capability of being suitable for both small and large number of samples, resulting therefore, perfectly suitable for diagnostic applications.

Since the highest achievable throughput is limited by the kinetic of the PCR reaction, optimization in the reaction buffer solution[32,55] can represent important perspectives for further improvements of this technology. Finally, the lower RNA amount considered for the calibration curve corresponds to the one of a single cell (about 15pg/drop), thus future outlooks include the coupling of this technology with a single cell-encapsulation device[56].

99

References

01 [1] J.A. Ludwig, J.N. Weinstein, Biomarkers in Cancer Staging, Prognosis and Treatment Selection, Nat. Rev.
02 Cancer. 5 (2005) 845–856. doi:10.1038/nrc1739.
03 [2] L.A. Garraway, J. Verweij, K. V Ballman, Precision oncology: an overview., J. Clin. Oncol. 31 (2013) 1803–
04 5. doi:10.1200/JCO.2013.49.4799.
05 [3] A.C. Wolff, M.E.H. Hammond, D.G. Hicks, M. Dowsett, L.M. McShane, K.H. Allison, D.C. Allred, J.M.S.
06 Bartlett, M. Bilous, P. Fitzgibbons, W. Hanna, R.B. Jenkins, P.B. Mangu, S. Paik, E.A. Perez, M.F. Press,
07 P.A. Spears, G.H. Vance, G. Viale, D.F. Hayes, American Society of Clinical Oncology, College of American
08 Pathologists, Recommendations for human epidermal growth factor receptor 2 testing in breast cancer:
09 American Society of Clinical Oncology/College of American Pathologists clinical practice guideline update.,
10 J. Clin. Oncol. 31 (2013) 3997–4013. doi:10.1200/JCO.2013.50.9984.
11 [4] E.A. Perez, A.C. Dueck, A.E. McCullough, M.M. Reinholz, K.S. Tenner, N.E. Davidson, J. Gralow, L.N.
12 Harris, L.A. Kutteh, D.W. Hillman, R.B. Jenkins, B. Chen, Predictability of adjuvant trastuzumab benefit in
13 N9831 patients using the ASCO/CAP HER2-positivity criteria., J. Natl. Cancer Inst. 104 (2012) 159–62.
14 doi:10.1093/jnci/djr490.
15 [5] D. Tvrdík, L. Staněk, H. Skálová, P. Dundr, Z. Velenská, C. Povýšil, Comparison of the IHC, FISH, SISH
16 and qPCR methods for the molecular diagnosis of breast cancer, Mol. Med. Rep. 6 (2012) 439–443.
17 doi:10.3892/mmr.2012.919.
18 [6] J. Jacquemier, F. Spyratos, B. Esterni, M.-J. Mozziconacci, M. Antoine, L. Arnould, S. Lizard, P. Bertheau,
19 J. Lehmann-Che, C.B. Fournier, S. Krieger, F. Bibeau, P.-J. Lamy, M.P. Chenard, M. Legrain, J.-M.
20 Guinebretière, D. Loussouarn, G. MacGrogan, I. Hostein, M.C. Mathieu, L. Lacroix, A. Valent, Y.M. Robin,
21 F. Revillion, M.L. Triki, A. Seaume, A.V. Salomon, P. de Cremoux, G. Portefaix, L. Xerri, S. Vacher, I.
22 Bièche, F. Penault-Llorca, SISH/CISH or qPCR as alternative techniques to FISH for determination of HER2
23 amplification status on breast tumors core needle biopsies: a multicenter experience based on 840 cases, BMC
24 Cancer. 13 (2013) 351. doi:10.1186/1471-2407-13-351.
25 [7] P.S. Bernard, C.T. Wittwer, Real-time PCR technology for cancer diagnostics, Clin. Chem. 48 (2002) 1178–
26 1185. doi:48.
27 [8] S. Mocellin, C.R. Rossi, P. Pilati, D. Nitti, F.M. Marincola, Quantitative real-time PCR: A powerful ally in
28 cancer research, Trends Mol. Med. 9 (2003) 189–195. doi:10.1016/S1471-4914(03)00047-9.
29 [9] S. Fleige, M.W. Pfaffl, RNA integrity and the effect on the real-time qRT-PCR performance, Mol. Aspects
30 Med. 27 (2006) 126–139. doi:10.1016/J.MAM.2005.12.003.
31 [10] J.S. Marcus, W.F. Anderson, S.R. Quake, Parallel picoliter RT-PCR assays using microfluidics, Anal. Chem.
32 78 (2006) 956–958. doi:10.1021/ac0513865.
33 [11] S.-Y. Teh, R. Lin, L.-H. Hung, A.P. Lee, Droplet microfluidics, Lab Chip. 8 (2008) 198.
34 doi:10.1039/b715524g.
35 [12] M.T. Guo, A. Rotem, J.A. Heyman, D.A. Weitz, Droplet microfluidics for high-throughput biological assays,
36 Lab Chip. 12 (2012) 2146. doi:10.1039/c2lc21147e.

[13] C.N. Baroud, F. Gallaire, R. Dangla, Dynamics of microfluidic droplets, Lab Chip. 10 (2010) 2032. doi:10.1039/c001191f.

[14] K.D. Dorfman, M. Chabert, J.-H. Codarbox, G. Rousseau, P. de Cremoux, J.-L. Viovy, Contamination-Free Continuous Flow Microfluidic Polymerase Chain Reaction for Quantitative and Clinical Applications, Anal. Chem. 77 (2005) 3700–3704. doi:10.1021/AC050031I.

[15] Y. Schaerli, R.C. Wootton, T. Robinson, V. Stein, C. Dunsby, M.A.A. Neil, P.M.W. French, A.J. deMello, C. Abell, F. Hollfelder, Continuous-Flow Polymerase Chain Reaction of Single-Copy DNA in Microfluidic Microdroplets, Anal. Chem. 81 (2009) 302–306. doi:10.1021/ac802038c.

[16] Y. Zhang, P. Ozdemir, Microfluidic DNA amplification—A review, Anal. Chim. Acta. 638 (2009) 115–125. doi:10.1016/J.ACA.2009.02.038.

[17] V. Taly, D. Pekin, L. Benhaim, S.K. Kotsopoulos, D. Le Corre, X. Li, I. Atochin, D.R. Link, A.D. Griffiths, K. Pallier, H. Blons, O. Bouché, B. Landi, J.B. Hutchison, P. Laurent-Puig, Multiplex Picodroplet Digital PCR to Detect KRAS Mutations in Circulating DNA from the Plasma of Colorectal Cancer Patients, Clin. Chem. 59 (2013) 1722–1731. doi:10.1373/CLINCHEM.2013.206359.

[18] R. Yang, A. Paparini, P. Monis, U. Ryan, Comparison of next-generation droplet digital PCR (ddPCR) with quantitative PCR (qPCR) for enumeration of Cryptosporidium oocysts in faecal samples, Int. J. Parasitol. 44 (2014) 1105–1113. doi:10.1016/J.IJPARA.2014.08.004.

[19] R. Arvia, M. Sollai, F. Pierucci, C. Urso, D. Massi, K. Zakrzewska, Droplet digital PCR (ddPCR) vs quantitative real-time PCR (qPCR) approach for detection and quantification of Merkel cell polyomavirus (MCPyV) DNA in formalin fixed paraffin embedded (FFPE) cutaneous biopsies, J. Virol. Methods. 246 (2017) 15–20. doi:10.1016/J.JVIROMET.2017.04.003.

[20] D. Dobnik, D. Štebih, A. Blejec, D. Morisset, J. Žel, Multiplex quantification of four DNA targets in one reaction with Bio-Rad droplet digital PCR system for GMO detection, Sci. Rep. 6 (2016) 35451. doi:10.1038/srep35451.

[21] B.T. Lau, C. Wood-Bouwens, H.P. Ji, Robust Multiplexed Clustering and Denoising of Digital PCR Assays by Data Gridding, Anal. Chem. 89 (2017) 11913–11917. doi:10.1021/acs.analchem.7b02688.

[22] J.F. Huggett, S. Cowen, C.A. Foy, Considerations for digital PCR as an accurate molecular diagnostic tool., Clin. Chem. 61 (2015) 79–88. doi:10.1373/clinchem.2014.221366.

[23] B. Shu, C. Zhang, D. Xing, Highly sensitive identification of foodborne pathogenic Listeria monocytogenes using single-phase continuous-flow nested PCR microfluidics with on-line fluorescence detection, Microfluid. Nanofluidics. 15 (2013) 161–172. doi:10.1007/s10404-013-1138-4.

[24] J. Chen, Z. Luo, L. Li, J. He, L. Li, J. Zhu, P. Wu, L. He, Capillary-based integrated digital PCR in picoliter droplets, Lab Chip. 18 (2018) 412–421. doi:10.1039/C7LC01160A.

[25] P. Mary, L. Dauphinot, N. Bois, M.-C. Potier, V. Studer, P. Tabeling, Analysis of gene expression at the single-cell level using microdroplet-based microfluidic technology, Biomicrofluidics. 5 (2011) 024109. doi:10.1063/1.3596394.

[26] N.R. Beer, E.K. Wheeler, L. Lee-Houghton, N. Watkins, S. Nasarabadi, N. Hebert, P. Leung, D.W. Arnold, C.G. Bailey, B.W. Colston, On-Chip Single-Copy Real-Time Reverse-Transcription PCR in Isolated Picoliter Droplets, Anal. Chem. 80 (2008) 1854–1858. doi:10.1021/AC800048K.

[27] Y. Zhu, Y.-X. Zhang, W.-W. Liu, Y. Ma, Q. Fang, B. Yao, Printing 2-dimentional droplet array for single-cell reverse transcription quantitative PCR assay with a microfluidic robot., Sci. Rep. 5 (2015) 9551. doi:10.1038/srep09551.

[28] K. Matsuda, A. Yamaguchi, C. Taira, A. Sueki, H. Koeda, F. Takagi, M. Sugano, T. Honda, A novel high-speed droplet-polymerase chain reaction can detect human influenza virus in less than 30 min, Clin. Chim. Acta. 413 (2012) 1742–1745. doi:10.1016/J.CCA.2012.06.026.

[29] M. UEHARA, K. MATSUDA, M. SUGANO, T. HONDA, A New High-Speed Droplet-Real-Time Polymerase Chain Reaction Method Can Detect Bovine Respiratory Syncytial Virus in Less than 10 Min, J. Vet. Med. Sci. 76 (2014) 477–480. doi:10.1292/jvms.13-0357.

[30] A. Rival, D. Jary, C. Delattre, Y. Fouillet, G. Castellan, A. Bellemin-Comte, X. Gidrol, An EWOD-based microfluidic chip for single-cell isolation, mRNA purification and subsequent multiplex qPCR, Lab Chip. 14 (2014) 3739–3749. doi:10.1039/C4LC00592A.

[31] M. Serra, D. Ferraro, I. Pereiro, J.-L. Viovy, S. Descroix, The power of solid supports in multiphase and droplet-based microfluidics: towards clinical applications, Lab Chip. 17 (2017) 3979–3999. doi:10.1039/C7LC00582B.

[32] T. Houssin, J. Cramer, R. Grojsman, L. Bellahsene, G. Colas, H. Moulet, W. Minnella, C. Pannetier, M. Leberre, A. Plecis, Y. Chen, Ultrafast, sensitive and large-volume on-chip real-time PCR for the molecular diagnosis of bacterial and viral infections, Lab Chip. 16 (2016) 1401–1411. doi:10.1039/C5LC01459J.

[33] A.C. Hatch, T. Ray, K. Lintecum, C. Youngbull, Continuous flow real-time PCR device using multi-channel fluorescence excitation and detection, Lab Chip. 14 (2014) 562–568. doi:10.1039/C3LC51236C.

[34] C.J. Hayes, T.M. Dalton, Microfluidic droplet-based PCR instrumentation for high-throughput gene expression profiling and biomarker discovery, Biomol. Detect. Quantif. 4 (2015) 22–32. doi:10.1016/J.BDQ.2015.04.003.

[35] Y. Schaerli, R.C. Wootton, T. Robinson, V. Stein, C. Dunsby, M.A.A. Neil, P.M.W. French, A.J. deMello, C. Abell, F. Hollfelder, Continuous-Flow Polymerase Chain Reaction of Single-Copy DNA in Microfluidic Microdroplets, Anal. Chem. 81 (2009) 302–306. doi:10.1021/ac802038c.

[36] D. Ferraro, M. Serra, D. Filippi, L. Zago, E. Guglielmin, M. Pierno, S. Descroix, J.-L. Viovy, G. Mistura, Controlling the distance of highly confined droplets in a capillary by interfacial tension for merging on-demand, Lab Chip. 19 (2019) 136–146. doi:10.1039/C8LC01182F.

[37] D. Ferraro, J. Champ, B. Teste, M. Serra, L. Malaquin, J.-L. Viovy, P. de Cremoux, S. Descroix, Microfluidic platform combining droplets and magnetic tweezers: application to HER2 expression in cancer diagnosis., Sci. Rep. 6 (2016) 25540. doi:10.1038/srep25540.

[38] D. Ferraro, M. Serra, I. Ferrante, J.-L. Viovy, S. Descroix, Microfluidic valve with zero dead volume and negligible back-flow for droplets handling, Sensors Actuators B Chem. 258 (2018) 1051–1059. doi:10.1016/J.SNB.2017.12.002.

[39] P. Juskova, A. Ollitrault, M. Serra, J.-L. Viovy, L. Malaquin, Resolution improvement of 3D stereo-lithography through the direct laser trajectory programming: Application to microfluidic deterministic lateral displacement device, Anal. Chim. Acta. 1000 (2018) 239–247. doi:10.1016/J.ACA.2017.11.062.

[40] T.D. Mai, D. Ferraro, N. Aboud, R. Renault, M. Serra, N.T. Tran, J.-L. Viovy, C. Smadja, S. Descroix, M.

Taverna, Single-step immunoassays and microfluidic droplet operation: towards a versatile approach for detection of amyloid-β peptide-based biomarkers of Alzheimer's disease, Sensors Actuators B Chem. 255 (2018) 2126–2135. doi:10.1016/j.snb.2017.09.003.

[41] D. Ferraro, Y. Lin, B. Teste, D. Talbot, L. Malaquin, S. Descroix, A. Abou-Hassan, Continuous chemical operations and modifications on magnetic γ-Fe $_2$ O $_3$ nanoparticles confined in nanoliter droplets for the assembly of fluorescent and magnetic SiO $_2$ @γ-Fe $_2$ O $_3$, Chem. Commun. 51 (2015) 16904–16907. doi:10.1039/C5CC07044A.

[42] D.Y. Wu, L. Ugozzoli, B.K. Pal, J. Qian, R.B. Wallace, The Effect of Temperature and Oligonucleotide Primer Length on the Specificity and Efficiency of Amplification by the Polymerase Chain Reaction, DNA Cell Biol. 10 (1991) 233–238. doi:10.1089/dna.1991.10.233.

[43] S. Taylor, M. Wakem, G. Dijkman, M. Alsarraj, M. Nguyen, A practical approach to RT-qPCR—Publishing data that conform to the MIQE guidelines, Methods. 50 (2010) S1–S5. doi:10.1016/J.YMETH.2010.01.005.

[44] J.-W. Pan, C.-M. Wang, H.-C. Lan, W.-S. Sun, J.-Y. Chang, Homogenized LED-illumination using microlens arrays for a pocket-sized projector, Opt. Express. 15 (2007) 10483. doi:10.1364/OE.15.010483.

[45] G. Wang, L. Wang, F. Li, D. Kong, Design of optical element combining Fresnel lens with microlens array for uniform light-emitting diode lighting, J. Opt. Soc. Am. A. 29 (2012) 1877. doi:10.1364/JOSAA.29.001877.

[46] S.A. Bustin, V. Benes, J.A. Garson, J. Hellemans, J. Huggett, M. Kubista, R. Mueller, T. Nolan, M.W. Pfaffl, G.L. Shipley, J. Vandesompele, C.T. Wittwer, The MIQE guidelines: minimum information for publication of quantitative real-time PCR experiments., Clin. Chem. 55 (2009) 611–22. doi:10.1373/clinchem.2008.112797.

[47] R.G. Rutledge, C. Côté, Mathematics of quantitative kinetic PCR and the application of standard curves, Nucleic Acids Res. 31 (2003) 93e – 93. doi:10.1093/nar/gng093.

[48] J.L. Gevertz, S.M. Dunn, C.M. Roth, Mathematical model of real-time PCR kinetics, Biotechnol. Bioeng. 92 (2005) 346–355. doi:10.1002/bit.20617.

[49] M. Kubista, J.M. Andrade, M. Bengtsson, A. Forootan, J. Jonák, K. Lind, R. Sindelka, R. Sjöback, B. Sjögreen, L. Strömbom, A. Ståhlberg, N. Zoric, The real-time polymerase chain reaction, Mol. Aspects Med. 27 (2006) 95–125. doi:10.1016/j.mam.2005.12.007.

[50] T.D. Schmittgen, K.J. Livak, Analyzing real-time PCR data by the comparative CT method, Nat. Protoc. 3 (2008) 1101–1108. doi:10.1038/nprot.2008.73.

[51] S.C. Taylor, G. Laperriere, H. Germain, Droplet Digital PCR versus qPCR for gene expression analysis with low abundant targets: from variable nonsense to publication quality data, Sci. Rep. 7 (2017) 2409. doi:10.1038/s41598-017-02217-x.

[52] A.K. White, M. VanInsberghe, O.I. Petriv, M. Hamidi, D. Sikorski, M.A. Marra, J. Piret, S. Aparicio, C.L. Hansen, High-throughput microfluidic single-cell RT-qPCR, Proc. Natl. Acad. Sci. 108 (2011) 13999–14004. doi:10.1073/pnas.1019446108.

[53] M. VanInsberghe, H. Zahn, A.K. White, O.I. Petriv, C.L. Hansen, Highly multiplexed single-cell quantitative PCR, PLoS One. 13 (2018) 1–18. doi:10.1371/journal.pone.0191601.

[54] D.W. Green, R.H. Perry, Perry's chemical engineer handbook, 8th edition, 2007.

[55] J.S. Farrar, C.T. Wittwer, G. Reed, J. Cherry, Extreme PCR: efficient and specific DNA amplification in 15-60 seconds., Clin. Chem. 61 (2015) 145–53. doi:10.1373/clinchem.2014.228304.

[56] D.J. Collins, A. Neild, A. deMello, A.-Q. Liu, Y. Ai, The Poisson distribution and beyond: methods for microfluidic droplet production and single cell encapsulation, Lab Chip. 15 (2015) 3439–3459. doi:10.1039/C5LC00614G.

Acknowledgment

This work was supported by the French National Research Agency (ANR) as part of the "Investissements d'Avenir" program (reference: ANR 10-NANO 0207), by the Labex and Equipex IPGG (references: 10-LABX-0031 and 10-EQPX-0034), by ERC "CellO" (FP7-IDEAS-ERC-321107) and by the ARC foundation for young researcher fellowship (DF). IH was supported by PhD founding from Fondation Pierre-Gilles de Gennes. MS was supported by a Curie Institute International PhD fellowship.

Conflict of interest

DF, MS, J-LV and SD are co-inventors of a patent application filed by Institut Curie and CNRS, encompassing some of the technologies described in this article.